# Mass Spectroscopic Study of the Chemical Reaction Zone in Detonating Liquid Nitromethane

**Normand C. Blais, Ray Engelke,* and Stephen A. Sheffield**

*Los Alamos National Laboratory, MS P952, Los Alamos, New Mexico 87545*

*Received: June 12, 1997*[⊗]

We report a time-of-flight mass spectroscopic study of the chemical reaction zone in base-sensitized detonating liquid nitromethane (NM--$CH_3NO_2$). Mass spectra of the reaction zone region are presented for cases where the $CH_3NO_2$, $^{13}CH_3NO_2$, and $CD_3NO_2$ forms of NM were detonated. In experiments in which detonation was made to occur, the detonation process was initiated by a slapper detonator system. The NM explosives were confined in steel, and the charge geometry was chosen such that the detonations were traveling steadily by the time the detonation wave reached the end of the charge. Various nondetonation control experiments were also performed and are described. Two-dimensional numerical fluid-dynamic computations that mimic the experimental system were performed in order to help in the interpretation. We estimate that, for the base-sensitized NM explosive used, the steady two-dimensional chemical-reaction zone is ca. 50 $\mu$m in spatial extent and has a time duration of ca. 7 ns. The most important result obtained is that the new chemical species that are observed in the reaction zone are the result of condensation reactions where two or more NM molecules combine to form molecules more massive than NM or produce molecules in which numerous nitrogen atoms are present. A brief review of earlier work on this problem is presented to aid readers in understanding the new results.

## I. Introduction

We report a time-of-flight (TOF) mass spectroscopic study of the chemical-reaction zone and following flow in detonating base-sensitized liquid nitromethane. Nitromethane, (NM)--$CH_3NO_2$, the simplest nitroalkane, is a clear water-white liquid with mass density 1.13 g/cm$^3$ at 25 °C; it is a moderately energetic insensitive high explosive and monopropellant. With normal handling, it can be treated as a solvent. Strong organic bases (e.g., diethylenetriamine (DETA), $NH_2(CH_2)_2NH(CH_2)_2$-$NH_2$) are known to sensitize NM to detonation significantly.[1]

We wished to study the reaction chemistry in a NM-based explosive under conditions in which it was actually detonating. In an effort to keep our experimental results as simple as possible, the geometry of our detonating samples was chosen such that the detonation flow was steady and had axial symmetry. This choice reduced the complexity of the fluid mechanics involved and, consequently, simplified the interpretation of the experimental data. Our sample geometry consisted of right-circular cylinders of explosive 3 mm diameter × 12 mm long confined in steel; this ratio of length to diameter assured that a steady two-dimensional axisymmetric detonation wave and reaction zone had been established by the time the detonation shock encountered the end of the charge.

The mass spectrometer used in our experiments has been described in detail elsewhere.[2] Its main useful features for studying the chemistry of detonation in condensed-phase explosives are (1) it allows one to detonate significant amounts of explosive (ca. ⩽ 0.5 g) in a high vacuum, (2) (and most significantly) the strong rarefaction wave reflected into the reacting material, when the detonation wave reaches the front surface of the charge, produces a very rapid quenching of the chemistry occurring in the charge, (3) this rarefaction wave takes time to travel back into the charge so the sequential layers of the charge (that the rarefaction wave encounters and quenches) give a record of the chemistry that has occurred as a function of space and time, and (4) these various layers are led collisionlessly into an electron beam ionizer, ionized, and directed through a TOF mass spectrometer to detectors where their mass composition is detected and recorded.

There have been many studies of the chemical kinetics that take place in reacting NM and base-sensitized NM; see section II. Some of these studies have been used to hypothesize what may be the initial important kinetics steps in these explosives when they are detonating. These hypotheses required long inferences from mechanical observations or were made from observations of microscopic events (e.g., vibrational spectra) that were far from the thermodynamic states that occur in detonating materials.

Here we report a direct study of the chemistry of detonating base-sensitized NM. The inferences we require in order to make statements about the chemical kinetics occurring in the detonation reaction zone are more direct than those required in the earlier studies.

Our primary results are that (1) the reaction zone in detonating 95/5 wt % NM/DETA is quite short, its spatial and temporal dimensions being ca. 50 $\mu$m and 7 ns for the fast early chemistry, and (2) (and possibly most important) we find evidence that *a condensation reaction*[3] *(or reactions) is (are) the first step(s) we are able to observe in the fast reaction zone chemistry.* We have reached these conclusions via a set of experiments in which the mass spectra of detonating protonated, deuterated, and $^{13}$C-labeled NM doped with DETA were obtained and analyzed. Various other ancillary and control experiments on nondetonating materials were also done to determine various cracking patterns and to clarify the experiments in which detonation occurred.

## II. Background

The literature on the chemical kinetics that occurs in NM and base-sensitized NM is very large, and consequently, we cannot review it exhaustively. Below, we briefly discuss some of the papers we think will familiarize the reader with the

[⊗] Abstract published in *Advance ACS Abstracts,* October 1, 1997.

S1089-5639(97)01928-2 CCC: $14.00 

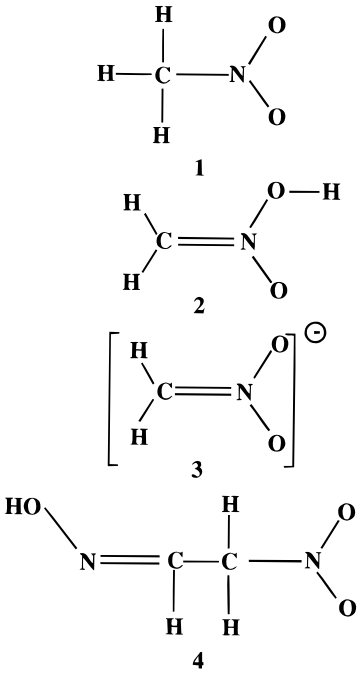

**Figure 1.** NM and various other molecular structures that play a role in NM chemistry. The structures are normal NM (**1**), the aci form of NM (**2**), the aci ion of NM (**3**), and methazonate acid (**4**).

complexity of this subject. We have restricted our discussion to experimental studies on neat NM and NM with small amounts of base present. We hope that this material will bring the reader to the realization that many different reaction schemes occur in NM depending on the mass density of the reacting material and the pressure and temperature histories it experiences.

**(a) Pure and Base-Sensitized NM Kinetics: Ambient Pressure.** There is agreement between workers that the initial kinetic step in the pyrolyses of gaseous NM is the homolytic breaking of the CN bond (see, e.g., ref 4 and references therein); the activation energy for this reaction is ca. 56 kcal/mol, which is close to the CN bond energy. Note that homolytic bond-breaking processes have positive volumes of activation and, thus, are hindered by pressure.[5]

Wang et al.[6] found a similar result applies to condensed-phase NM even at pressures up to 0.01 GPa when the degree of reaction is <20%.

When bases are added to liquid NM, first the NM aci ion (see Figure 1) is produced followed by a reaction that produces the methazonate ion.[7] Methazonate acid (i.e., the protonated form of the ion) has the structure $O_2NCH_2CHNOH$ (see Figure 1). Since the formation of methazonate acid (1) is a condensation reaction and is, therefore, accelerated by pressure, (2) produces water (a detonation product), and (3) is significantly exothermic, we thought that, perhaps, this structure or a remnant of it would show up in our detonation mass spectra. This seems not to be the case. It is still possible that the methazonate reaction is important in the detonation chemistry but that it occurs too rapidly to be seen with our instrument.

**(b) Pure and Base-Sensitized NM Kinetics: Static High Pressure.** Wang et al.[6] found that with applied static pressure in the range 0.7−1.1 GPa the NM decomposition mechanism (in toluene solution) changes from CN bond breaking to one accelerated by pressure (with a volume of activation of ca. −5.5 $cm^3$/mol at 23 °C). These workers also found qualitatively similar results when 2-nitropropane was studied but qualitatively dissimilar results when 2,2-dinitropropane was examined. Note that 2-nitropropane has an acid or "aci" form (as does NM; see Figure 1), whereas 2,2-dintropropane does not. This suggests that the aci form or the aci ion of nitroalkanes plays some role in the condensed-phase high-pressure chemical kinetics of nitroalkanes.

Lee et al. made observations on the time to explosion of condensed-phase NM in a heatable high-pressure cell.[8] They found that the time to explosion of NM was *decreased* when the pressure was increased from 1 to 5 GPa; this is evidence that the initial step in the kinetics scheme has a *negative* volume of activation in this pressure/temperature region. Their experiments on 2,2-dinitropropane showed a *positive* volume of activation. In similar experiments, Shaw et al. found that for deuterated NM the time to explosion is ca. 10 times longer than that of the protonated material.[9] This suggests that a proton or hydrogen atom abstraction is involved in the rate-determining step. Engelke et al., via isotope-exchange experiments that used diamond cell methods, gave evidence that increased pressure increases the aci ion concentration.[10] They suggested that Lee et al.'s observation of a reduced time to self-explosion at high pressure is due to the increased aci ion presence.

Piermarini et al. studied NM's decomposition kinetics in a diamond cell in the pressure and temperature ranges 2.0−7.1 GPa and 120−180 °C.[11] They found that pressure speeds up the decomposition process in their entire pressure range, indicating a negative volume(s) of activation. Interestingly, their results show three distinct kinetic regimes as a function of pressure and temperature.

Brasch did diamond cell reaction studies of NM pressurized from 2.0 to 5.0 GPa and at temperatures from 100 to 160 °C.[12] He noted that the observed reactions occurred more rapidly when 1% of ethylenediamine was added to the NM in the diamond cell.

Naud and Brower did thermolysis studies of NM/piperidine mixtures in THF solution at 1 GPa and 125 °C and found the decomposition to be pressure enhanced.[13] They suggested that the probable mechanism of the base-catalyzed decomposition involves a bimolecular reaction of the aci-nitroalkane with the nitroalkane aci ion (see Figure 1).

**(c) Pure and Base-Sensitized NM Kinetics: Shock Wave Studies.** Various shock wave studies have been made on pure and base-sensitized NM. Here we restrict ourselves to a few of the experimental studies that have some direct implication on the underlying chemical kinetics. Recovery experiments are not discussed because of their inherent complexity.

Winey[14] has studied pure NM shocked to final pressures between 12 and 19 GPa and temperatures up to ca. 725 °C. These experiments used a shock "ring-up" process in which a thin NM sample is multiply shocked between two sapphire windows; this process leads to a much lower temperature than would be achieved in a single shock experiment to the same pressure. Three vibrational modes of the NM molecule were observed during the shock process via their Raman Stokes lines. All three vibrations show hardening (i.e., they are shifted to higher frequency) at high pressure. An increase in the noise background was seen, and this was interpreted as possibly being due to chemiluminesence that was indicative of chemical reaction(s). An irreversible shift in an electronic transition band edge was also seen when the final "ring-up" pressure was 17 GPa. This background signal and band-edge shift are non-specific in terms of defining the chemicals species involved in the initial kinetic steps in reacting NM.

A conclusion was drawn from this work that there is no pressure effect on the chemical kinetics observed (neither an acceleration nor a deceleration). This is in contrast to all the static high-pressure results discussed above, i.e., other work performed in the condensed phase at pressures above 0.7 GPa.

The probable explanation is that all of Winey's ring-up kinetics observations were made at such high ring-up pressures that the $\int_{v_0^{\pm}}^{v_f^{\pm}} P\ \mathrm{d}(\Delta v^{\pm})$ term in the exponential of $\exp[-(\Delta E^{\pm} + \int_{v_0^{\pm}}^{v_f^{\pm}} P\ \mathrm{d}(\Delta v^{\pm}))/kT]$ had already reached its asymptotic value at all the pressures observed.

It is of interest to compare the physical state and reaction time scales observed in Winey's experiments with the conditions that occur in detonating liquid NM. Detonating liquid NM's Chapman−Jouguet (CJ) pressure[15] is ca. 13 GPa, and the "spike" pressure is probably ca. 15 GPa. The temperature in the reaction zone is less well-known but is thought to be ca. 1800 K at the von Neumann spike. The highest temperature reached in any of the ring-up experiments was ca. 725 °C. Thus, while the measurements were made in a pressure range (i.e., 12−19 GPa) similar to those in the detonating material, the maximum temperatures reached were roughly a factor of 2 lower than the temperature characteristic of an NM detonation. Also, in Winey's experiments, it takes ca. 120 ns to reach full pressure, while in the reaction of detonating NM, maximum pressure is reached in less than 1 ns. Therefore, the ring-up experiments, while interesting, were not conducted in the same thermodynamic regime or on the same time scale as occurs in the detonation reaction zone of NM.

There have been many shock wave studies of base-sensitized NM. The earliest such study, to our knowledge, is ref 16. Further studies that examined the quantitative response of NM detonation to the amount of base present are those in ref 1. In ref 1a, a working hypothesis was advanced that the aci ion of NM (see Figure 1) is the principal sensitization agent; this idea was supported by showing that the UV sensitization of NM to detonation was correlated with aci ion presence.[17]

Constantinou et al.[18] did optical absorption measurements on "rung-up" NM similar to those of Winey described above, but with base sensitizer added to the NM (0.1 mol % ethylenediamine). They saw irreversible changes in their samples in an experiment whose final state was 482 °C and 13.2 GPa; this possibly indicates a new reaction path has been induced by the amine. Similar experiments by Gupta et al.[19] were also done, using Raman scattering as the diagnostic. Evidence of reaction was again obtained at ca. 14 GPa and 480 °C. They interpreted their data as being evidence of homolytic CN bond breaking. This cannot be correct, however, since a $CH_3$ stretch at 2968 $cm^{-1}$ and an $NO_2$ stretch at 1400 $cm^{-1}$ (which are both characteristic of the NM molecule) persist relatively unaffected in the spectra.

**(d) Assessment**. One obtains the impression from the works discussed in this section that the chemical kinetics of condensed-phase NM for pressures greater than ca. 0.7 GPa may involve a number of kinetics routes and that the operative routes can be accentuated or hindered by varying the pressure and temperature regimes experienced; evidently, there is no simple single reaction scheme that can explain all the observations. As might be expected for such an energetic material, the dominant reactions can change dramatically with changes in the pressure−density−temperature state variables.

One result of the accumulated knowledge cited above is that the high-pressure kinetics of interest is pressure-enhanced. Two reaction classes that have this character are bimolecular reactions involving neutral species (e.g., aldol condensations) and reactions that involve the production of ions.[20] These classes are merely examples and are not necessarily the operative kinetics paths in liquid NM detonation.

A prime motivation of a significant portion of the papers cited above was to cast light on the chemical kinetics that takes place in the detonation of NM. However, the combined results do not lead to a clear picture. Furthermore, none of the reported work directly (or even closely) examines the chemistry of the detonating material. In view of this and of our having access to a research instrument (the LANL detonation mass spectrometer) with which such an examination could be made, we undertook the research described below.

## III. Experimental Apparatus, Techniques, and Materials

The major components of the detonation mass spectrometer are the following: (1) A large volume high-vacuum chamber in which the explosive charge is detonated; the molecular species in the detonating material are rapidly expanded into the high vacuum of this chamber. (2) A portion of this expanding material travels through a "skimmer" into an even higher vacuum region and is formed into a molecular beam. (3) This beam is then subjected to a 90 eV electron beam that ionizes part of it. (4) The ionized portion is then directed (approximately transversely to its original motion) by electric fields onto two microchannel plate detectors that record the intensity vs time data. The ionizing electron beam is applied to the molecular beam for 1 $\mu$s every 12 $\mu$s. The time interval it takes a molecule to reach the detectors determines its mass. The mass spectrometer is fully described in ref 2, and the characteristics of the slappers used to initiate the explosives are described in ref 21. Only special features of the equipment used in the current experiments are described in detail below.

We have made mass spectral measurements of NM and chemically sensitized NM in three different situations: (1) with the sensitized NM detonating steadily in a cell (see Figure 2), (2) with the sensitized NM shocked but not initiated in the same type of cell, and (3) with both pure NM and sensitized NM formed into a molecular beam in a free-jet expansion from a nozzle. The same mass spectrometer and mass spectrometric conditions were used in all three types of experiments.

We wished to study the detonation of NM in the liquid phase because of the relative simplicity of the detonation process in a homogeneous explosive[22] and because all earlier shock wave studies of the material have been done in the liquid state. To do such an experiment in the detonation mass spectrometer, we developed the cell shown in Figure 2.

NM's vapor pressure is 4 kPa (30 Torr) at ambient temperatures; this makes isolation of the liquid from the evacuated region a necessity. The cell shown in Figure 2 is simple in its final appearance, but it required considerable design effort before we reached this final version. Previous detonation studies with liquid NM sensitized to the degree used here indicated that the failure diameter of the material is ca. 50 $\mu$m when it is fired in a thick steel right-circular cylinder at ambient temperature; therefore, any explosive diameter greater than ca. 100 $\mu$m is a satisfactory charge size for the sensitized NM when fired in steel cells. For pure liquid NM, the same value is 1.9 ± 0.5 mm fired at 25 °C. For the detonation reaction zone to become steady in this geometry requires that the detonation wave run ca. four charge diameters.[23] Due to these considerations, we chose to make our explosive charge reservoir in the cell a right-circular cylinder 3 mm diameter × 12 mm long. This gave a manageable charge size for our apparatus and at the same time assured that the detonation wave speed (and reaction zone structure) was constant when the wave reached the exit seal. In addition, we wanted to preserve the cylindrical geometry of the expanding detonation products that we had used in our previous detonation studies of solid explosives (see ref 24). Therefore, we decided that "gluing" the sealing material to the steel surfaces adjacent to the detonation volume of the cell was desirable rather than trying to devise bulkier mechanical seals.

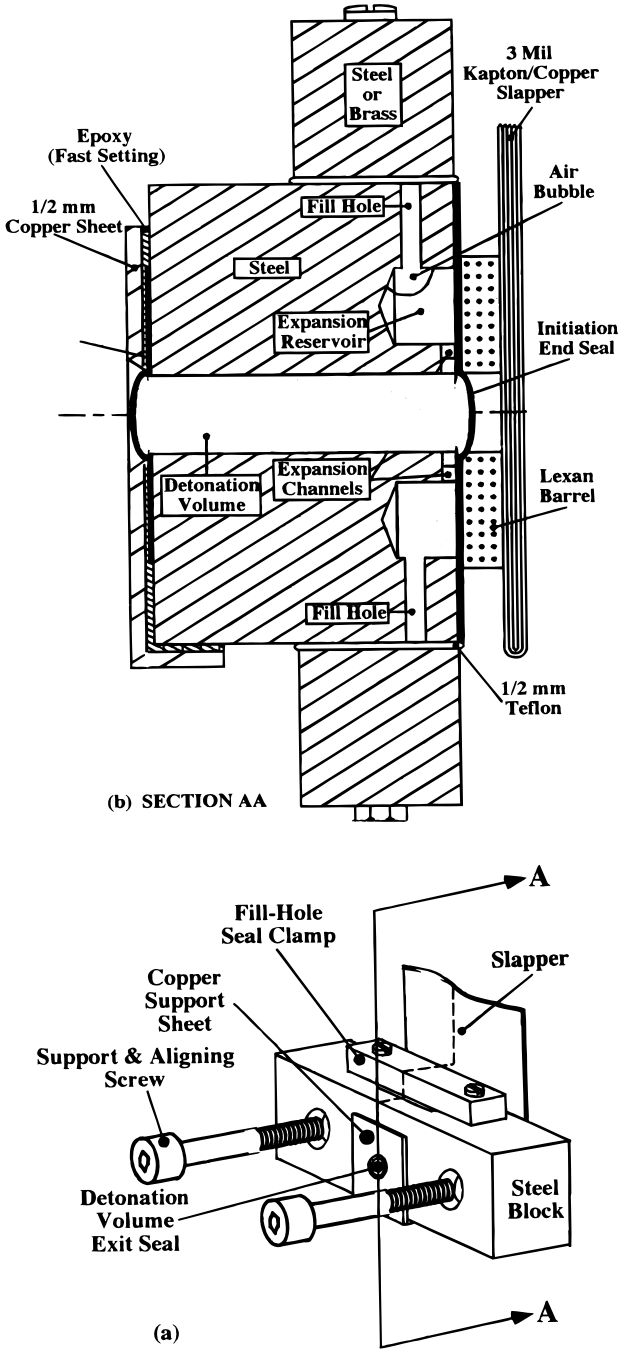


**Figure 2.** (a) Assembly used to contain and detonate the NM explosive within the mass spectrometer vacuum chamber. The assembly is approximately drawn to scale. (b) Section AA cut of the assembly shown in (a). Major features illustrated are the detonation chamber, its expansion reservoirs, and the slapper detonator/barrel assembly used to initiate the charge. The steel blocks were 51 mm wide × 19 mm high × 12 mm thick. The detonation volume was 3 mm diameter × 12 mm long. The front and initiation end Kapton seals were 12.7 and 76.2 $\mu$m thick, respectively. The Kapton slapper thickness was 76.2 $\mu$m, and the barrel length was 3 mm.

Steel was an obvious choice for the cell body. We chose Kapton film as the seal material for the ends of the cells and "Epoxi-Patch"[25] adhesive to glue the Kapton to the steel cell faces. Most of our experiments used 12.7 $\mu$m thick Kapton film as the exit seal of the detonation volume (see Figure 2).

Two expansion reservoirs were drilled above and below the detonation volume and connected to that volume by a small channel (see Figure 2b). When filling the cell with explosive, we introduced a small bubble in the top reservoir before sealing the cell with the seal clamps. This was done to circumvent formation of bubbles in the detonation volume. The bubble introduced into the top reservoir forces liquid from the expansion reservoir into the detonation chamber to replace liquid lost by diffusion through and expansion of the Kapton windows. We found it expedient to passivate the cell with pure NM overnight under vacuum before filling it with the charge to be detonated.

We were able to examine each cell (with a telescope through a large viewing port in the mass spectrometer vacuum chamber) just prior to detonating it. If bubbles or other anomalies that could alter the symmetry of the detonation wave were seen, the charge was not fired.

In most of our experiments, the NM was sensitized by adding 5 wt % DETA (3.1 mol %). Steel plate dent tests with a mock-up of our cell showed that this degree of base sensitization is sufficient to lead to detonation of the charge with our slapper initiation system.

We found that our initiation system was not sufficiently powerful to initiate some NM explosives in the steel cell. For example, 100% $CH_3NO_2$ could not be initiated, even though the charge was larger than its failure diameter; this was an initiation problem due to the Kapton flyer thickness. $CD_3NO_2$ failed to initiate when the DETA concentration was $\leqslant$0.5 wt %; this is probably due to a kinetic isotope effect that slows the detonation chemical kinetics, similar to that seen by Shaw et al. in self-explosion experiments.[9]

We list the following experimental parameters to provide a sense of the energies involved in detonating NM, along with the energy necessary to initiate the process. All energies are in joules: the slapper capacitive discharge unit stored energy ($^1/_2CV^2$) of 338 with the 12 $\mu$F unit charged to 7.5 kV, the heat of detonation of 0.1 g of NM is 445, and the Kapton flyer had a kinetic energy of ca. 11 when its parameters were $\rho_0 = 1.414$ g/cm$^3$, diameter = 3 mm, thickness = 75 $\mu$m, and speed = 5.5 km/s.

All of the NM samples, (protonated, deuterated, and $^{13}$C labeled) were used as received from the manufacturer without further purification.[26] Purity was checked using GC/MS and found to be within supplier's specifications of 99 wt % purity.

We obtained mass spectra under free-jet expansion conditions in order to identify any ions in the detonation spectra that arise simply from the electron impact ionizer of the mass spectrometer acting on the NM and/or DETA molecules. The heatable nozzle source described in ref 21 was modified slightly to allow the reagent samples to be placed externally to the main detonation vacuum chamber. In this way, we were able to conveniently examine the mass spectra of various mixtures of NM and DETA under different expansion conditions. The samples examined ranged from pure $CH_3NO_2$ and $CD_3NO_2$, to 95/5 wt % NM/DETA, and up to 50/50 wt % NM/DETA. Helium was used as the carrier gas. The nozzle conditions ranged from mild expansions, where only parent molecules were present in the molecular beam, to more vigorous expansions, where clusters of the molecular species were clearly present.

Figure 3 illustrates two such nozzle spectra. The top panel is of pure DETA taken with a sample temperature of ca. 75 °C, a nozzle temperature of 115 °C, and a He carrier stagnation pressure of ca. 15 kPa (200 Torr). The bottom panel shows a spectrum of pure $CH_3NO_2$ at about the same He gas pressure, but at a sample temperature of 23 °C and a nozzle temperature of 110 °C. Both molecules are seen to fragment extensively upon electron impact ionization. Note that reasonably strong ion peaks of both species (which are located in a mass region free of final detonation products) are present, i.e., a fragment at mass 73 for DETA and the parent mass 61 for NM.

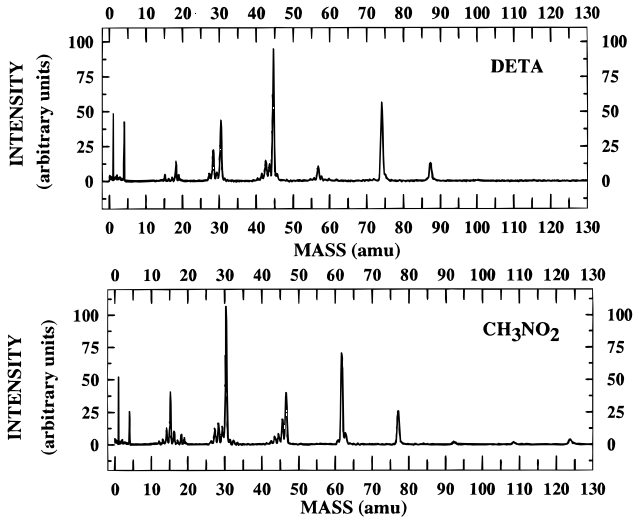


**Figure 3.** (a, top panel) The cracking pattern of the base diethylenetriamine (DETA) obtained by expansion of the material through a nozzle into the mass spectrometer. Three hundred scans were coadded to obtain this (low-noise) spectrum. (b, bottom panel) A similar nozzle-expansion spectrum of nitromethane (NM) obtained by coadding 96 scans of the spectrometer. Note that there is evidence of the presence of NM multimers as seen in the lines at 76 $[(CH_3NO_2)_2$ minus $NO_2]^+$ and in the small peaks at even higher mass.

We chose operating conditions for the mass spectrometer such that the ions of particular interest to us appeared mostly on the multichannel plate (MCP) detector downstream along the initial molecular beam direction. (We denote this detector as MCP2; see ref 2.) The two microchannel plates are identical objects—each having an active collecting area of 44 mm diameter and a gain of ca. 1 million. MCP2 is in the same plane as MCP1, but is downstream of it, along the molecular beam direction. The edges of the two detectors are ca. 6 mm apart.

We found that the time−mass calibration differed perceptibly between the MCP1 and MCP2 detectors. Calibration of MCP1 is routinely done with a nozzle beam,[2] but this procedure cannot be used with the MCP2 detector. Consequently, we made a special effort to calibrate the mass scale for MCP2 under conditions as nearly identical with the shot conditions as possible. A molecular beam of high-velocity sulfur clusters was useful for this calibration, in particular the $S_3$ and $S_4$ clusters. The procedure for forming the beam is described in ref 2, and a sample sulfur spectrum is shown there also.

## IV. Fluid Dynamic Modeling of the Experiments

The CTH wave propagation code[27] was chosen to do the fluid dynamic modeling of the experiments. CTH is a mixed Eulerian/Lagrangian code. That is, the problem is set up in the Eulerian frame and then mapped to the Lagrangian frame where the fluid motion is calculated for one time step. The results are then mapped back into the Eulerian frame. This process is repeated for the each new time step of the calculation. This methodology eliminates some of the problems associated with cell distortion, etc., experienced with pure Eulerian codes.

All the calculations were done in two-dimensional cylindrical geometry with the problem set up as close as possible to the experimental setup. A 11 mm diameter steel cylinder 12 mm long with a 3 mm diameter hole surrounded the NM explosive charge. The steel cylinder had a 75 $\mu$m thick Kapton initiation end seal on it (see Figure 2), and the NM was initiated with a 3 mm diameter, 75 $\mu$m thick Kapton flyer moving at a velocity of 5.5 mm/$\mu$s. The impact of the flyer on the seal drove a 26 GPa shock wave into the Kapton seal. When this shock wave reached the lower impedance NM, a 22 GPa shock was generated in the NM; this caused a very rapid initiation of the NM. The von Neumann spike pressure in detonating NM is ca. 15 GPa, so this input strongly overdrives the NM. A heavy brass tamper was placed at the rear of the slapper assembly to mimic our arrangement for holding the sample cell. It was separated from the steel and NM by a 2 mm thick Kapton barrel (which had a 3 mm diameter hole in it).

To simulate the initiation of the NM and then the resulting detonation wave in the NM, we used a global (single reaction) rate form. The global reactive model controlled the conditions under which the unreacted NM was converted into reaction products. We chose the HVRB (history variable reactive burn) model,[28] which is a pressure-dependent rate model with a time delay in the onset of reaction. Specifically, the reaction starts slowly and builds as a function of time. The extent of reaction progress variable $\lambda$ is given by

$$\lambda = \min(1,\varphi^M), \quad \phi = \frac{1}{\tau_0}\int_0^t \left(\frac{P - P_i}{P_r}\right)^z \mathrm{d}\tau$$

where $M$, $P_r$, $P_i$, and $z$ are adjustable parameters calibrated for a particular explosive, and $\tau_0$ is chosen to be 1 $\mu$s to make $\lambda$ dimensionless. $\lambda$ varies from 0 for no reaction to 1 for full reaction, and $P$ is the local pressure in the NM. This model is typically calibrated to simulate explosive initiation experiments in which time and distance to detonation are measured for a particular shock input.

The unreacted NM equation of state (EOS) used was a Mie−Gruneisen form (based on the shock properties) with a constant specific heat and mass density times Gruneisen parameter product. The NM reaction product EOS was a tabular form and was based on a mixture chemical equilibrium model that simulates detonation cylinder expansion experiments.[29]

Cell zones were rectangular with the zone size 30 $\mu$m in both the radial and axial directions. This led to calculations with up to 260 000 cells. However, even with this many cells, some of the features (such as the Kapton flyer, NM reaction zone, etc.) were spread out over only a few cells. This, along with the artificial viscosity necessary to stabilize the calculations, led to wave profiles that were not sharply defined as will be seen from some of the figures shown below. The calculations took up to 24 h to complete on a HP-735 workstation.

The EOS used to describe the Kapton was a Mie−Gruneisen form with the same assumed properties as used for the NM EOS (i.e., constant specific heat and constant value of the product of the mass density and Gruneisen parameter). Tabular EOSs available within the CTH code[27] were used to describe the steel and brass parts of the assembly.

The Kapton flyer initiated a detonation wave in the NM that propagated down the axis as a reactive wave with properties similar to an actual detonation in NM; i.e., the reaction zone was resolved. This calculated reactive wave is shown in Figure 4. The front of the shock wave is not sharp because of the finite cell size and the need for artificial viscosity. However, the wave is a reasonable simulation of an actual detonation wave in NM.

When the detonation wave interacts with the end of the NM column, a strong rarefaction is reflected back into the reacting NM which rapidly erodes the pressure state produced by the detonation wave. The passage of this rarefaction wave freezes the chemistry, so the mass spectrometer samples the chemical species generated in the NM reaction zone. Figure 5 shows the wave shapes produced by the rarefaction/detonation wave interaction at Lagrangian positions 30, 60, and 90 $\mu$m back from

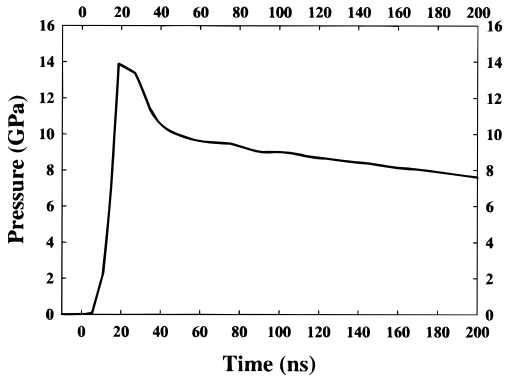


**Figure 4.** Computer simulation of the detonation wave in NM at a position of 10 mm down the axis from the flyer plate input. Some smearing of the wave is evident because of the cell size and the artificial viscosity of the code. In this simulation, the von Neumann spike is about 14 GPa and the reaction zone about 20 ns.

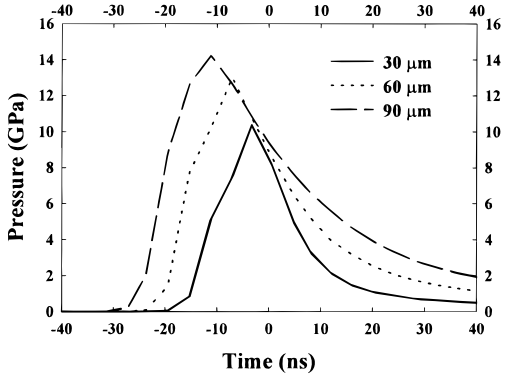


**Figure 5.** Computer-generated pressure histories of Lagrangian particles 30, 60, and 90 $\mu$m back from the NM/vacuum interface. The particles at 30 and 60 $\mu$m positions do not achieve the full 14 GPa of the detonation wave because they are smeared out by the finite cell size and artificial viscosity. The time above a particular pressure is, however, indicative of the detonation wave/rarefaction interaction that occurs after the detonation wave interacts with the interface.

the interface. In this figure time has been zeroed to the time of wave interaction with the surface. Because of the finite cell size and artificial viscosity, the wave profiles nearer the surface are somewhat spread out and do not achieve the full von Neumann spike pressure. However, they do indicate that the wave is rapidly quenched by the rarefaction and give an indication of the time the material is held at pressure, if we take 6 GPa as the pressure at which the NM stops reacting. The reaction times for Lagrangian particles initially 30, 60, and 90 $\mu$m back from the front are ca. 12, 22, and 32 ns, respectively. We think these times are overestimates because of the calculational wave smearing. The particles nearer the surface would be expected to have times shorter than these estimates.

In the actual experiments, the end of the NM had a 12.7 $\mu$m thick Kapton layer to hold the NM in place. We ran various NM calculations with different thicknesses of Kapton on the end, but because we could not simulate a reaction pyrolyzing the Kapton, which would be expected to take place when the detonation wave interacts with it, it was felt that the best simulation would be without a Kapton layer. The profiles in Figure 5 are from such a calculation.

In the actual experiments, the reacting material expands out of the steel column as shown in Figure 6. These pictures were taken using Schlieren methodology; therefore, their form is determined by the mass density gradient rather than the mass density. To get some idea of how the simulation was comparing to the actual experiments, we used the CTH graphics analysis

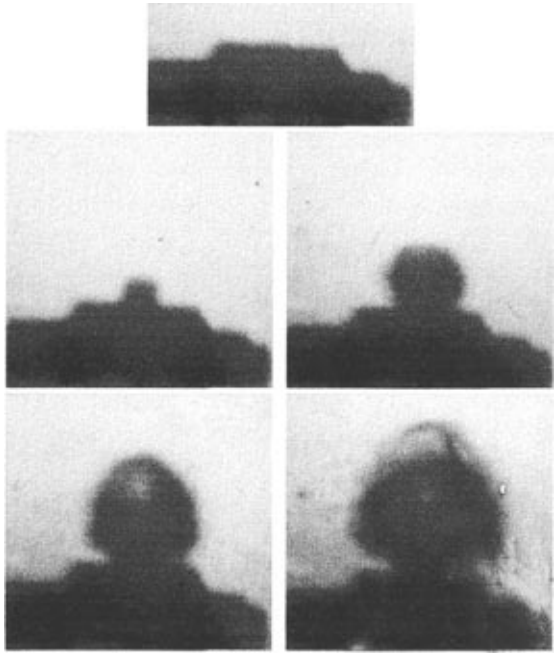

**Figure 6.** Schlieren photographs of the shot shown in Figure 8; the composition of this shot was 95/5 wt % $CD_3NO_2$/DETA. The light source used was an EG&G xenon strobe unit Model MVS 2020. It had a total capacity of 36 $\mu$F and provided a single pulse 20 $\mu$s wide at half-maximum. The image was obtained with an Imacon 790 framing camera and $10^6$ frames-per-second amplifier module. ASA 3000 speed Polaroid film was used to record the image. Both entrance and exit apertures were 1 mm diameter. The parallel light section of the optical path, at the object, was about 8 cm diameter. Frames shown are (top) before breakout, (middle left) near breakout, (middle right) ca. 1 $\mu$s after breakout, (bottom left) ca. 2 $\mu$s after breakout, and (bottom right) ca. 3 $\mu$s after breakout.

package to provide a picture of the expanding material that is similar to what would be produced by an X-ray of the experiment. This picture (Figure 7) can be compared with the right middle schlieren picture of Figure 6, which was taken at approximately the same time.

An interesting side issue in Figure 7 is the rings above the metal surface (one is at a "Y" position of ca. 1.4 cm in the picture). These are rings of steel that have spalled from around the inside diameter confining the NM. The shock interactions are such that these metal rings move out from the steel surface. Inspection of the steel blocks from the actual experiments indicates that such spalling is probably occurring. This is an indication that the calculations are mimicking the experiments reasonably well.

## V. Experimental Results

**(a) Detonation Mass Spectra.** The time-dependent mass spectra of the detonation products of NM are central to this work; therefore, we show such a set of spectra in Figure 8. Five consecutive scans are shown, each spaced 12 $\mu$s apart (the first scan is started by the trigger signal which starts the slapper current pulse), starting with scan 13. The explosive charge, in this case, consisted of deuterated NM ($CD_3NO_2$) sensitized with 5 wt % DETA. We show this spectrum because it displays interesting features to which we want to call attention and which we will discuss below. Where necessary, the spectra shown are the coadded signals from MCP1 and MCP2.

The first scan shown in Figure 8 (i.e., scan 13) starts 144 $\mu$s after the initiating voltage pulse was applied to the slapper detonator, so that the products entering the mass spectrometer ionizer had a speed of about 9 km/s and a kinetic energy of

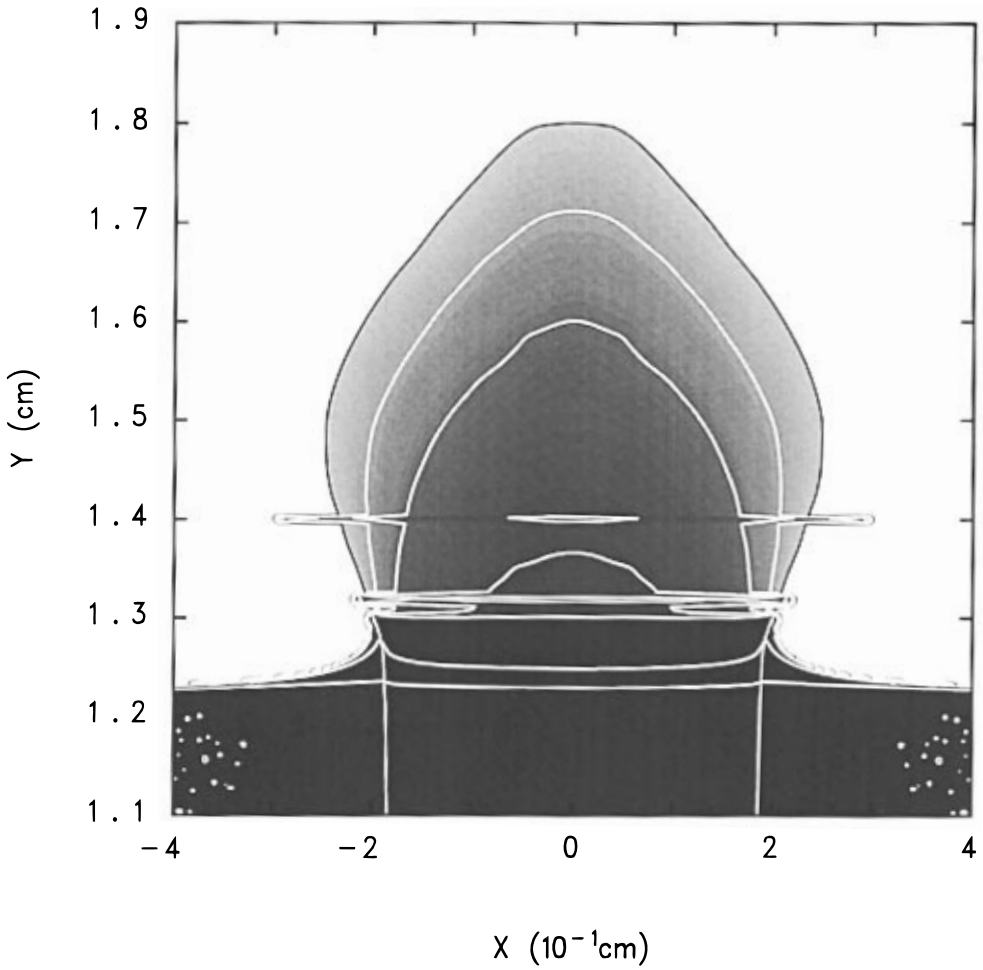


**Figure 7.** CTH graphic of the material coming out of the steel cylinder at a time 1 $\mu$s after the detonation wave interacts with the free surface. The shading is the result of doing a linear density mass sum in the radial direction. The outer contour is at a linear mass density of 0.005 g/cm$^3$, and other contours at 0.01, 0.02, 0.05, 0.1, 0.5, and 2.0 g/cm$^3$ are also shown. Shading also starts at 0.005 g/cm$^3$ and goes to a maximum at 0.1 g/cm$^3$. The rings that are apparent (the most prominent one is at the $Y = 1.4$ cm position) are due to wave interactions that cause the steel to spall from the inside diameter of the steel confining the NM.

nearly 0.4 eV/amu. Mostly light masses with relatively low intensity are seen in scan 13; these consist of atomic ions and masses 20, 28, and 44. Two small features at $m = 60$ and 120 also appear. We have occasionally seen these peaks in other spectra upon arrival of the first ions; we think they are molecular fragments from the pyrolyzed Kapton exit seal.

Scans 14 and 15 are the most interesting of the series that follow. In these, the number density of the products rises rapidly, and the complexity of each spectrum increases. Ions of the low heat of formation ($\Delta H_f$) detonation products (e.g., $N_2$, CO, $CO_2$, $H_2O$) become prominent, but of special importance is the appearance of ions of unreacted NM and other, mostly more massive species. All of these latter ions disappear in subsequent scans. Scans 14 and 15 show the mass spectra of molecules that have come from the region of the detonated charge called the "reaction zone".[15] Scans that follow, (i.e., scan 16 and later) also display large spectral features, but mostly at masses lower than $m = 46$ (i.e., the low $\Delta H_f$ detonation product species).

Two ions in particular that are heavier than the parent ion of $CD_3NO_2$ ($m = 64$) grow in on scans 14 and 15, i.e., $m = 76$ and a broad signal at $m = 106-110$. We attribute these ions to reaction intermediates of the exoergic reactions that lead from $CD_3NO_2$ to the low $\Delta H_f$ final reaction products of the detonation.

The small "zero-signal" spots near the center of each of the spectra in Figure 8 are a result of our data analysis; see, for example, the mass range 45−50 amu in scan 14. Because of our chosen operating conditions, ions of the masses in the blank regions actually strike the circular MCP detectors near the boundary separating the two plates. The detector sensitivity functions in this region (which we use to normalize the MCP signals) are very small (i.e., $\leqslant 0.2$); that is, the detectors are very insensitive to real signals. Because of this we "zeroed" any data when the value of either sensitivity function was less than 0.2.

A total of 17 detonated shots of NM were fired, of which 9 were with protonated NM, 6 were with deuterated NM, and 2 were $^{13}C$ labeled. All but one of these spectra exhibited mass spectroscopic features that we interpret as coming from the reaction zone. These features always occurred in the first two, or at most three, scans that followed the arrival of beam molecules at the mass spectrometer detectors. This onset occurred reproducibly at 144 $\mu$s after initiation, provided the cell exit seals were as shown in Figure 2. Out of the remaining set of 16 shots, 14 showed clearly resolvable ion signals that we attribute to reaction intermediates; the reaction intermediate signals were too small to work with in two shots. Five of these detected mass values have sufficient intensity to warrant particular examination and are discussed below. When the explosive charge was $CH_3NO_2$, these five masses were $m =$ 58, 73, 86, 104, and 207. These masses have several important features in common. First, they only appear in the reaction zone scans. Second, they do not appear in spectra of NM or mixtures

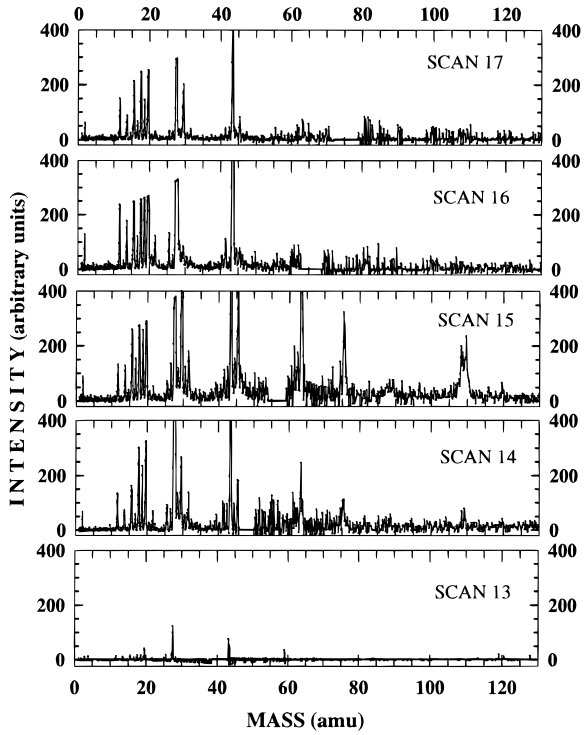


**Figure 8.** Mass spectra from a shot in which 95/5 wt % $CD_3NO_2$/DETA material was used. The sequence of scans starts just as masses begin to arrive at the detectors (scan 13) and proceeds through the scans in which the reaction zone molecular species are evident (scans 14 and 15) to scans in which only the detonation products are strongly evident (scans 16 and 17). Note, particularly, the strong broad peak between 106 and 110 and the strong deuterated NM peak (mass = 64) in scan 15.

of NM/DETA, except when the sample detonated. Third, most of these ions have masses that are considerably larger than that of NM. Note that the mole fraction of DETA present was too low for us to see any of its ion signatures.

Not all five of the reaction intermediates appeared in any one spectrum. However, a pattern was evident. If $m = 58$ was prominent in the spectrum, as it was in four of the shots, the other intermediates were almost always absent. The heavier ions appeared more often, in 10 of the spectra, and often together. The masses $m = 86$ and $m = 207$ also appeared in this group of 10, but only four times. This suggests that these ions are not electron-impact fragments of a common parent molecule.

A number of factors may be causing this lack of reproducibility in our observations. One cause is probably the space and time resolution the mass spectrometer is capable of in its present configuration and that we are testing the limits of this ability when studying sensitized NM. We are sequentially observing ca. 20 $\mu$m layers of our NM charges, and the reaction zone of unsensitized NM is only a few multiples of this number.[2] Another factor, which is completely out of our control, is that there are known to be Mach stem structures (of very fine space scale in sensitized NM) present in the reaction zone of detonating NM explosives[30] which will "force" the chemical kinetics locally. Since we are only looking at a small area on our charge face, at least some of the lack of reproducibility may be traceable to this source.

We have not yet obtained a good experimental measurement of the relative depth in the detonating medium displayed between successive scans of the mass spectrometer. We estimated earlier[2] that each successive scan comes from ca. 20 $\mu$m deeper in the charge. This suggests that the reaction zone for sensitized NM is 40−60 $\mu$m long under our conditions.

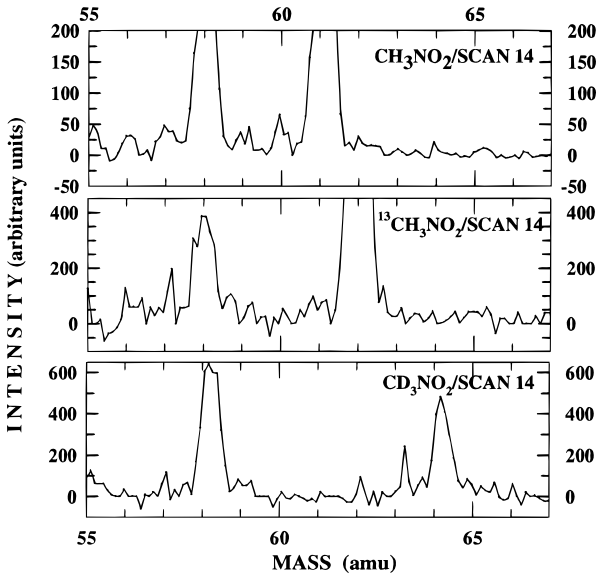


**Figure 9.** Spectra in the mass range 55−67 amu for three shots that used $CH_3NO_2$ (top panel), $^{13}CH_3NO_2$ (middle panel), and $CD_3NO_2$ (bottom panel) molecules. Note the mass shift in the NM lines due to the labeling. Most importantly, note that the line at mass 58 does not shift with isotopic labeling; the only structure consistent with these spectra is $N_3O^+$.

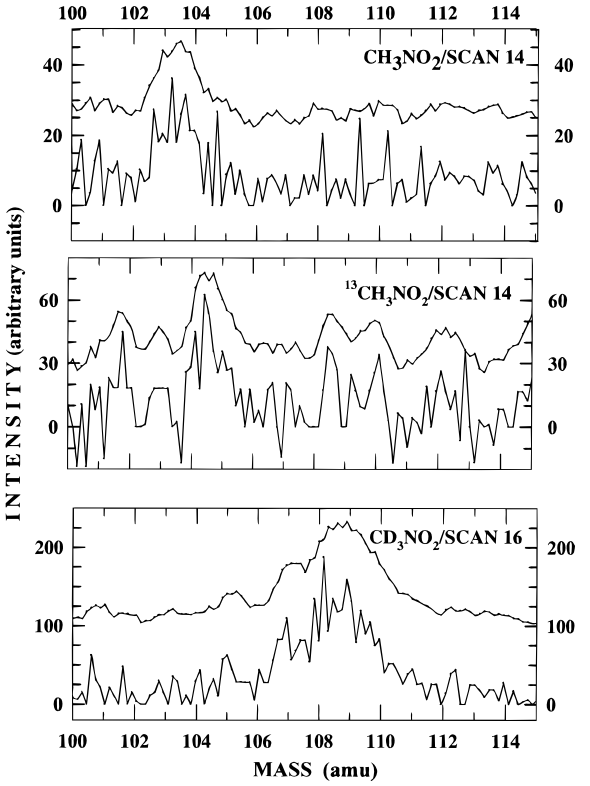


**Figure 10.** Mass spectra in the mass range 100−115 amu for three shots that used $CH_3NO_2$ (top panel), $^{13}CH_3NO_2$ (middle panel), and $CD_3NO_2$ (bottom panel) molecules. Two points are important: (1) the mass shift in the line positions due to isotopic labeling and (2) the increased peak width of the heavy species for the deuterated NM case. Both the raw data and data that have been subjected to a five-point running average are shown. The five-point running fit values have been offset by 20, 30, and 100 intensity units on the $CH_3NO_2$, $^{13}CH_3NO_2$, and $CD_3NO_2$ panels, respectively.

**(b) Reaction Intermediates.** More detailed views of the mass spectral scans in the regions around two of the most interesting reaction intermediates are shown in Figures 9 and 10. Figure 9 shows the ion with mass 58, and Figure 10 shows

that with mass in the range 104−110. One scan is shown for each of the three differently isotopically labeled NM charges. The top panels of the two figures are for $CH_3NO_2$, the middle panels are for $^{13}CH_3NO_2$, and the bottom panels are for $CD_3NO_2$. A five-point running averaging algorithm was used to smooth out some of the noise in the data in Figure 10, but the raw data are also shown.

Figure 9 shows both the 58 amu ion and the NM parent ions. This is the only reaction intermediate we found with mass less than NM. It has a particularly simple stoichiometry. It is clear that the ion does not contain either hydrogen or carbon since the mass is the same for each of the three spectra. The stoichiometry is unique; i.e., the only possible molecular formula is $N_3O^+$.

Another reaction intermediate ion that we were able to assign a stoichiometry is shown in Figure 10. The mass for this species falls in the range 104−110 depending on the labeled atoms. The resulting mass shifts upon isotopic labeling were clearly observable in the shots for which the ions appeared.

The data indicate that the mass shift in the heavy species arising from the $CH_3NO_2$ and $^{13}CH_3NO_2$ materials is ca. 1 mass unit; therefore, the species contains one carbon atom. Because of the importance of this observation, we based it on a quantitative estimate of the shift in the centers of gravity of the two signals. To estimate the centers of gravity, the raw data were integrated with the trapezoidal rule over a 2.5 amu span centered approximately at the line centers. The centers of mass for the $CH_3NO_2$ and $^{13}CH_3NO_2$ peaks were found to be at 103.49 and 104.65, respectively. The masses are not at integer values because of electrooptical and space charge effects that distort the molecular beam in its travel from the ionizer to the detectors. Because of this, it is not possible to calibrate the machine's mass scale exactly over the entire mass range.

For this species, it is evident that the deuterated ion signals are considerably broader than the corresponding peaks in the panels for $CH_3NO_2$ and $^{13}CH_3NO_2$, so that the mass shift upon deuteration is thereby more difficult to define. Some of the broadening arises because 14% of the hydrogens in the NM explosive charge came from the undeuterated DETA base; this is due to exchange of the five labile hydrogens on the amine groups with the hydrogens on $CD_3NO_2$ via the aci form and aci ion of NM (see Figure 1 and ref 10). This causes the deuterated ion signal to broaden in the direction of lower mass. However, our analysis indicates that this accounts for only part of the observed width. Apparently, the deuterated ion is not that of the parent molecule but is a fragment resulting from the ionization process in the mass spectrometer ionizer. The simplest fragmentation process is either H or $H_2$ (D or $D_2$) elimination. If H or $H_2$ is eliminated, it occurs rapidly enough that the time-of-flight is relatively unaffected, and the observed ion mass is that of the parent minus the eliminated fragment. However, if deuterium is eliminated, it takes long enough to separate that the ion traverses a significant portion of the ion accelerating region of the mass spectrometer during the elimination process. The observed ion mass is then that of the parent molecule minus a fraction of the eliminated fragment mass; that fraction depends on where in the ion accelerating region the fragmentation was complete. We estimate a separation time for D or $D_2$ of about 0.4−0.5 $\mu$s. Dissociative ionization of this type is well-known in mass spectrometry.[31]

We can assign a stoichiometry for each of the two fragmentation schemes. If H (and therefore also D) is eliminated, then the parent ion of the observed signal is $CH_5N_4O_2$, and it has mass 105 for $CH_3NO_2$ and 110 for $CD_3NO_2$. If $H_2$ ($D_2$) is eliminated, then the parent molecule is $CH_4N_3O_3$, and it has mass 106 for $CH_3NO_2$ and 110 for $CD_3NO_2$. Because single H atom fragmentation is the most frequently observed of these dissociative ionization events, we favor the first scheme.

Definite isotopic shifts between $CH_3NO_2$ and $CD_3NO_2$ were found for the other three designated reaction intermediates. The signals for these ions were too small with $C^{13}$ labeling to determine the carbon number. With $CD_3NO_2$ the $m = 73$ peak shifted to $m = 76$ (see Figure 8). In the case of $m = 86$, the $CD_3NO_2$ signal shifted and increased in width to $m = 88-90$, much as we observed with the $m = 104-110$ ion. Assuming a hydrogen elimination, then the mass of the parent molecule would be $m = 87$ for $CH_3NO_2$ and $m = 90$ for $CD_3NO_2$. There are thus several possible stoichiometries for these ions: for $m = 73$ there are three, i.e., $H_3N_5$, $CH_3N_3O$, and $C_2H_3NO_2$. Similarly, $m = 87$ has three possibilities, i.e., $H_3N_6$, $C_3H_3O_3$, and $CH_3N_4O$. As previously noted, the ion at $m = 73$ is not from DETA remnants of the initial charge as a shot fired with 1/10 of the DETA concentration gave equivalent signals.

We did not attempt to determine the atomic makeup of the $m = 207$ ion. It would have required a significant effort to overcome a combination of difficulties with the mass calibration in that mass range and with the reduced mass resolution at high mass. We do call attention, however, to the fact the mass of this ion is nearly double that of the reaction intermediate at $m = 105$.

We are confident that all of the parent molecules that lead to the ions we discussed above are reaction intermediates arising from the chemical kinetics that occurs in the reaction zone of the detonating materials. These ions are not due to ion−molecule or intracluster reactions in the mass spectrometer ionization region, since we did not observe any of these species under any experimental conditions with NM and DETA, except when the reagents detonated.

**(c) Schlieren Photography.** The first five frames of a series of schlieren photographs[32] are shown in Figure 6. The cell shown in Figure 2 is shown in side-view silhouette in Figure 6. Breakout occurred shortly before frame 2.

The pictures show that the product expansion is quite symmetric, at least in the plane of the photograph. There are no observable plumes or whiskers coming from the leading edge of the product cloud. The first few frames show that the expansion is highly directional along the axis of the apparatus, and only at frame 5 does the radial expansion start to compete with the longitudinal flow. For frames 2, 3, and 4 we have approximately measured the axial expansion speed of the front of the product cloud; we find it is about 8 mm/$\mu$s. This compares well with the speeds of the products shown in scans 14 and 15 of Figure 8.

The resolution for these photographs was ca. 2 mrad minimum ray deflection. Apparently, there are parts of the expansion in frames 4 and 5 in which the *net* deflection of the light rays is less than 2 mrad, and bright regions are seen behind the thin dark leading edge of the expansion. This shows that there is little solid carbon in that part of the expansion and that the film darkening is because of light-ray deflection and not absorption. This also agrees with our mass spectra, since we see little evidence of any carbon clustering.

## VI. Conclusions and Discussion

We can make two statements about the results of these experiments: (1) our apparatus is able to detect some of the reacting molecular species present in the reaction zone of detonating liquid NM, and (2) the nature of these species is evidence that they are the result of *condensation* reactions of some type.[3]

Earlier results of experiments using this apparatus were reported by Greiner et al., who described reaction zone products from the detonation of pressed pellets of TATB.[24] They too included isotopically labeled material to identify some of these products. Their results and ours are the only experimental reports we know of that identify molecular constituents (i.e., species that are reaction intermediates) in the reaction zone of any condensed-phase explosives during detonation. We point out that the reaction zone of NM is much shorter than that of high-density solid TATB, about 50 $\mu$m as compared to ca. 3 mm.

The identity of all of the reaction intermediates that we report here show that their atomic constituents came from two or more NM molecules. Moreover, the baseline of our reaction zone spectra in the mass range 61−250 amu was consistently cluttered with unresolvable and low-intensity ions. These too are most likely reaction intermediates, but with too low a concentration to be analyzable. As with our identified intermediates, they were present only in the reaction zone scans. This indicates that the chemical reactions from which they came are at least bimolecular and may include termolecular or higher order reactions. This conclusion is seen to be reasonable if we bear in mind that the density of the fluid in the reaction zone is ca. 30% higher than that of the initial charge density. This implies that some of the intermolecular distances approach the intramolecular bond lengths. NM molecules, as well as large intermediates, are effectively "caged" by their surrounding fluid constituents. Thus, the probability of repeated encounters between them is increased considerably as compared to lower density conditions. Condensation reactions can thus become the dominant reaction mechanism. At lower densities, such reactions would be less important because faster reactions involving electrically neutral radical species (that are suppressed by high pressure) would dominate. Because the diffusion length is also much shorter at high densities, the radical mechanisms are made less important than at low densities because any radicals are also caged. Furthermore, model calculations[33] have also shown that high densities can also lead to enhanced reactivity because many-body effects can lower the activation barriers of bimolecular or higher order reactions on the reaction potential energy hypersurface. Hopefully, more rigorous theoretical work will become available to verify the importance of many-body effects in chemical reactions such as those studied here.

As we described in the Background section, there is considerable evidence that the NM aci ion is important in the detonation chemistry of NM. But even though our apparatus conditions prevent detection of any charged species that originate in the detonating charge, this does not preclude the reaction intermediates we observe from being the products of reactions that involve such ionic species. We have decided not to conjecture about plausible detailed reaction mechanisms for the detonation process in NM, because our experimental data do not sufficiently constrain the problem to make such conjectures useful. The only requirements on observing reaction intermediates in our apparatus is that they be neutral by the time that molecular collisions cease in the product expansion and that they are energetically stable enough to survive the ca. 100 $\mu$s travel time from the breakout of the detonation to the mass spectrometer ionizer.

There is an important difference between our NM results and those of Greiner et al.'s work.[24] Most of the ions of the reaction intermediates in NM had masses heavier than the parent molecule of the explosive. In the TATB results only a few ions heavier than TATB were reported: a dimer of TATB and an unidentified ion at TATB + 26. The important species were at masses less than 50 amu. This difference may be partially attributable to instrumental effects. Ions with masses much heavier than that of TATB (258 amu) become more difficult to see because of the mass spectrometer sensitivity and resolution above that mass range. So while the TATB spectrum may have contained some reaction intermediates heavier than TATB, they were not easily seen. In the case of NM, we start out with a much lighter molecule so that the instrument is still reasonably sensitive for masses heavier than NM. Also in contrast to the TATB work, we found only one ion ($N_3O^+$), at 58 amu, that was lower in mass than NM that was not attributable to the expected stable reaction products of the detonation or to NM itself. Perhaps a careful quantitative study of the light mass region ($m$ < 61 amu) will reveal the presence of such species, but their concentrations will not be large. We intend to report such a study later to compare our mass spectra of the light mass stable products of NM detonation with those calculated with existing equilibrium chemical composition computer codes.

Each of the reaction intermediates we find can perhaps be formed at different stages of the reaction process. The fact that the 58 amu ion ($N_3O^+$) usually appears by itself indicates that it is not directly related to those other, heavier intermediate molecules that we have identified. It is clearly a species with a high heat of formation and therefore most likely an electron-impact fragment of some other, more metastable and higher mass parent. This could also be the case for some of our other identified intermediate species. With our limited time resolution we cannot make out the sequence in which the various reaction intermediates occur. With each individual shot our mass spectrometer picks out a slightly different time segment in the progression of the chemistry leading from NM reagent to final reaction products (e.g., due to jitter in our initiation system) so different reaction intermediates are observed in the various spectra.

**Acknowledgment.** This work was supported by the U.S. Department of Energy.

## References and Notes

(1) (a) Engelke, R. *Phys. Fluids* **1980**, *23*, 875. (b) Kondrikov, B. N.; Kozak, G. D.; Raikova, V. M.; Starshinov, A. V. *Dokl. Akad. Nauk SSSR* **1977**, *233*, 402 [*Sov. Phys. Dokl.* **1977**, *233*, 315].

(2) Blais, N. C.; Fry, H. A.; Greiner, N. R. *Rev. Sci. Instrum.* **1993**, *64*, 174.

(3) Fessenden, R. J.; Fessenden, J. S. *Organic Chemistry*, 2nd ed.; Willard Grant Press: Boston, 1982; pp 678−679.

(4) Crawforth, C. G.; Waddington, D. J. *Trans. Faraday Soc.* **1969**, *65*, 1334.

(5) Issacs, N. S. *Liquid Phase High Pressure Chemistry*; Wiley: New York, 1981; pp 203−208.

(6) Wang, J.; Brower, K. R.; Naud, D. L. Submitted to *J. Org. Chem*.

(7) (a) Brownstein, S. *J. Org. Chem.* **1963**, *28*, 2919. (b) Griswold, A. A.; Starcher, P. S. *J. Org. Chem.* **1965**, *30*, 1687.

(8) Lee, E. L.; Sanborn, R. H.; Stromberg, H. D. In *Fifth Symposium (International) Detonation;* Jacobs, S. J., Ed.; Office of Naval Research: Washington, DC, 1970; p 331.

(9) Shaw, R.; Decarli, P. S.; Ross, D. S.; Lee, E. L.; Stromberg, H. D. *Combust. Flame* **1979**, *35*, 237; **1983**, *50*, 123.

(10) Engelke, R.; Schiferl, D.; Storm, C. B.; Earl, W. L. *J. Phys. Chem.* **1988**, *92*, 6815.

(11) Piermarini, G. J.; Block, S.; Miller, P. J. *J. Phys. Chem.* **1989**, *93*, 457.

(12) Brasch, J. W. *J. Phys. Chem.* **1980**, *84*, 2084.

(13) Naud, D. L.; Brower, K. R. *High-Pressure Res.* **1992**, *11*, 65.

(14) Winey, J. M. Ph.D. Dissertation, Washington State University, Pullman, WA, 1995.

(15) Engelke, R.; Sheffield, S. A. *Encycl. Appl. Phys.* **1993**, *6*, 327.

(16) Eyster, E. H.; Smith, L. C.; Walton, S. R. U.S. Naval Ordnance Lab. Report No. NOLM 10336, 1949.

(17) Engelke, R.; Earl, W. L.; Rohlfing, C. M. *J. Phys. Chem.* **1986**, *90*, 545.

(18) (18) Constantinou, C. P.; Winey, J. M.; Gupta, Y. M. *J. Phys. Chem.* **1994**, *98*, 7767.

(19) Gupta, Y. M.; Pangilinan, G. I.; Winey, J. M.; Constantinou C. P. *Chem. Phys. Lett.* **1995**, *232*, 341.

(20) Engelke, R.; Pettit, D. R.; Sheffield, S. A. *J. Phys. Chem. A* **1997**, *101*, 1696.

(21) Engelke, R.; Blais, N. C. *J. Chem. Phys.* **1994**, *101*, 1096.

(22) Engelke, R.; Bdzil, J. B. *Phys. Fluids* **1983**, *26*, 1210.

(23) Campbell, A. W.; Engelke, R. In *Sixth Symposium (International) on Detonation*; Edwards, D. J., Ed.; Office of Naval Research: Washington, DC, 1976; p 642. An example is detonation speed data obtained from bare pellets of HMX, RDX, and HNS at 75% of their maximum theoretical density. These pellets were 3 mm diameter and 18 mm long and were initiated with a slapper detonator. The motion of the detonation wave along the charge length was photographed with a streak camera. The detonation wave speed (ca. 7000 m/s) was constant over the last third of the charge to within ca. ± 20 m/s.

(24) Greiner, N. R.; Fry, H. A.; Blais, N. C.; Engelke, R. *Tenth Symposium (International) on Detonation;* Office of Naval Research: Arlington, VA, 1993; pp 563−569.

(25) Epoxi-Patch is a trade name for a binary epoxy adhesive manufactured by the Dexter Corp., Adhesives and Structural Materials Division, 2850 Willow Pass Rd., Pittsburgh, CA 94565.

(26) Normal NM ($CH_3NO_2$) was purchased from J.T. Baker, Inc., Phillipsburg, NJ 08865. The isotopically labeled NMs were purchased from Sigma Chemical Co., P.O. Box 14508, St. Louis, MO 63178. All were specified to have at least 99% purity.

(27) McGlaun, M. C.; Thompson, S. L.; Kmetyk, L. N.; Elrich, M. G. A Brief Description of the Three-Dimensional Shock Wave Physics Code CTH, Sandia National Laboratories, SAND89-0607, 1989.

(28) Kerley, G. I. CTH Equation of State Package: Porosity and Reactive Burn Models, Sandia National Laboratories, SAND92-0553, 1992.

(29) (a) Kerley, G. I. Theoretical Equations of State for the Detonation Properties of Explosives. In *Proceedings of the Eighth Symposium (International) on Detonation*; Short, J. M., Ed.; Naval Surface Weapons Center: White Oak, MD, 1986; NSWL MP 86-194, pp 540−547. (b) Kerley, G. I. Theoretical Model of Explosive Detonation Products: Tests and Sensitivity Studies. In *Proceedings of the Ninth Symposium (International) on Detonation*; Morat,W. J., Ed.; Office of the Chief of Naval Research: 1990; OCNR 113291-7, pp 442−451. (c) Kerley, G. I.; Christian-Frear, T. L. Prediction of Explosive Cylinder Tests Using Equations of State from the PANDA Code, Sandia National Laboratories, SAND93-2131, 1993.

(30) Mallory, H. D. *J. Appl. Phys.* **1967**, *38*, 5302.

(31) (a) McLafferty F. W. *The Interpretation of Mass Spectra: An Introduction;* W. A. Benjamin, Inc.: New York, 1966. (b) Barnard, G. P. *Modern Mass Spectrometry*; The Institute of Physics: London, 1953.

(32) Saxe, R. F. *High-Speed Photography*; The Focal Press: London, 1966; p 86.

(33) Blais, N. C.; Stine, J. R. *J. Chem. Phys.* **1990**, *93*, 7914.